Study of charge carrier mobility in PBS nanocrystal layers using field-effect transistors

© P.S. Parfenov, N.V. Bukhryakov, D.A. Onishchuk, A.A. Babaev, A.V. Sokolova, A.P. Litvin

Center of Optical Information Technologies, ITMO University,
197101 St. Petersburg, Russia

E-mail: qrspeter@gmail.com

Received September 1, 2021
Revised October 15, 2021
Accepted October 15, 2021

The field-effect transistor method is used to study the mobility of charge carriers in layers of lead sulfide nanocrystals with ligands of tetrabutylammonium iodide and 1,2-ethanedithiol used to create solar cells. The difference between the operating of a transistor in ambient air and in an inert atmosphere is demonstrated. It is shown that, in the ambient air, the processes of charging nanocrystals are activated when current flows, and the influence of the polarization of the interface of nanocrystals and the insulator on the measurement of the mobility is analyzed. Different reactions of the layers with ligands to light have been demonstrated, showing a significant oxidation of the surface of nanocrystals treated with 1,2-ethanedithiol.

Keywords: solar cells, trap states, photoconductivity.

DOI: 10.21883/SC.2022.02.53049.9734

1. Introduction

Solar cells (SC) based on PbS nanocrystals are a popular direction in the development of photovoltaics. PbS nanocrystals (NCs) absorb in a wide spectral range and are characterized by a large Bohr radius, which makes it easy to implement the mode of strong quantum confinement and, hence, to select the desired optical properties. By changing the ligand molecules attached to the PbS NC surface, one can change the distance between the NCs, thus affecting the charge transfer between the NCs and the conductivity inside the layer, respectively [1], shift the position of the Fermi level and the band gap edges [2], which is necessary to match the levels in the energy structure of devices, as well as change the type of layer conductivity, making hole or electronic conductivity dominant. Although studies of such devices are carried out during manufacture in an inert atmosphere and subsequent operation in an encapsulated form, a number of studies show a rather high efficiency of such devices when operating in ambient air. It was established that exposure to air for several days leads to an improvement in SC parameters [3].

Processes occur in air in PbS NC layers, these processes significantly change their optical and physical characteristics. Thus, due to surface oxidation the effective NC diameter decreases, and the absorption and luminescence maxima are shifted, and the luminescence decay time also changes [4,5]. For the operation of optoelectronic devices it is more significant that the NC diameter may change during oxidation, and, consequently, the width of the intercrystal barrier may change, as well as the oxide phase and additional acceptor states of oxygen can also appear. Such appearance of new acceptor states can change the conductivity type of the layer. For example, it has been shown in several papers that ambient air exposure leads to a change in the type of conductivity of lead chalcogenide of NCs to a *p*-type, even if, due to treatment with ligands it was of *e*-type [1,6].

Models used to describe devices operating in air are currently based entirely on data obtained for devices manufactured in an inert environment. In our works we also proceeded from such a model [7,8]. At the same time it is clear that a complete description of the such devices operation, which is necessary for optimizing their operation, requires the determination of the band structure of layers, the concentration of charge carriers, their mobility, mean free path, and lifetime i.e. parameters that can vary significantly under action of the environment. In this paper we focus on the study of the charge mobility of PbS NC layers in air and put forward assumptions regarding the differences in the operation of solar cells based on them.

2. Experimental procedure

2.1. Solar cells based on PbS nanocrystals

In this paper we consider the functioning of SCs based on the structure using two layers of PbS NCs treated with ligands of 1,2-Ethanedithiol (EDT) and Tetrabutylammonium iodide (TBAI). Such ITO/ZnO/PbS−TBAI/PbS−EDT/Au structure is widely used, in it the formation of electron-hole pairs occurs in a layer of PbS−TBAI nanocrystals, charge separation occurs at the layers interface of ZnO/PbS−TBAI nanocrystals, while the PbS−EDT layer plays the role of holes transport and electrons blocking. The analysis of the processes occurring at the interface of layers in such elements is carried out in the papers [9–11].

To describe processes in SC layers, one usually studies the mobility of charge carriers, their concentration, the distribution of trap states, the position of Fermi levels, and

processes at the layer interfaces. In this paper we confine ourselves to considering the issue of charges mobility.

2.2. Determination of charge mobility by field-effect transistor method

To measure the mobility of charge carriers and determine the type of conductivity, we used the field-transistor method. In this method the substance under study forms a channel between the drain and the source, and the gate, separated from the channel by a dielectric layer, repels or attracts electrons and holes with its potential. This changes the carriers concentration, and, hence, changes the channel resistance and the current between drain and source. Analyzing the current dependence in the channel on the gate potential $I_{ds}(V_{gs})$, or the transfer characteristic (or current-gate voltage characteristic), one can determine the mobility of both electrons and holes. Depending on the point on the output characteristic $I_{ds}(V_{ds})$ (or drain characteristic), which shows the current in the channel vs. the voltage between the drain and source at a given gate potential, the linear mode and the saturation mode are separated, and the appropriate calculation formulas are applied [12].

The carriers mobility value is determined from the slope of the linear section of the transfer characteristic (holes according to *p*-channel transfer characteristic with a negative bias of gate and drain, electrons — according to *n*-channel transfer characteristic at positive bias of gate and drain). For the linear mode the mobility is defined as

$$\mu_{\text{lin}} = \frac{L}{WC_{ox}V_{ds}} \frac{\partial I_{ds}}{\partial V_{gs}}\bigg|_{V_{ds}=\text{const}},$$

where W is channel width, L is channel length, C_{ox} is insulator layer capacitance per unit area (oxide capacitance), μ is mobility.

The threshold voltage V_{th} corresponds to the end of the current exponential growth zone on the transfer characteristic, and the voltage of the beginning of the current exponential growth is called as onset voltage V_{on}, it corresponds to the beginning of channel formation. The values of V_{on} and V_{th} depend on various effects (interface states, traps and dipole states, impurities [13]). The most common reason for a nonzero turn-on voltage is charged trap states at the interface with a dielectric [14]. A significant turn-on voltage bias can be caused, for example, by polarization of the dielectric, and manifests itself as a hysteresis [13].

Note that the above formula is valid within the approximation (Gradual Channel Approximation), assuming the thickness of the channel is negligible compared to its length. In this case the electric field in the channel is uniform, and edge effects can be neglected. Therefore, an important moment in determining the mobility is the linearity of the selected section, since very often the inflection point of curves is taken as a linear section, which gives an overestimated value of mobility [12]. If the linear section cannot be reached in any mode, then the mobility must be calculated exclusively from the linear mode. This is due to the fact that the saturation mode is more prone to error, especially if the mobility depends on the concentration of charge carriers, which varies along the channel and may additionally depend on the band-tail filling [15].

2.3. Description of substrates

The work was carried out using Prefabricated OFET Test Chips substrates, supplied by Osilla, made on the basis of a highly doped silicon wafer with pre-deposited metal electrodes. Channel width — 1 mm, channel length — 30 μm, silicon oxide insulator thickness — 300 nm, insulator capacitance $1.09 \cdot 10^{-8}\,\Phi/\text{cm}^2$. An example of the substrates use is given in [16]. Since silicon oxide forms acceptor trap states, the manufacturer requires the substrates to be silanized, indicating the impossibility of investigating electron mobility otherwise.

The presence of many acceptor vacancies in silicon oxide and their influence on the operation of the transistor is a well-studied topic, for example, in the paper [17]. It is known that such states can lead to V_{th} increasing [18], and it was shown in paper [14] that a nonzero voltage V_{on} indicates the presence of charged trap states at the interface with the dielectric.

Work without silanization is possible, but will be associated with a very high turn-on voltage V_{TH}. Thus, the paper [19] shows V_{th} change from 41 and 13 V for electrons and holes, respectively, in the case of pure silicon oxide to 27 and -11 V after treatment with Hexamethyldisilazane (HMDS), which shows a significantly lower capture of electrons in traps. Comparison of six different silanes is carried out in [20], where the best electrons mobility is recorded with HMDS ($V_{\text{on-e}} = V_{\text{on-h}} = -5$ V), and the best mobility of holes, and at the same time the worst for electrons — with Dodecyltrichlorosilane. The article additionally shows that silanization is not at all a necessary step for the study of PbS NC samples, but the choice of a substance for silanization affects the results and can lead to a significant overestimation of mobility.

2.4. Investigation of the mobility of charge carriers

In the work we used PbS NCs with a diameter of 3.4 nm (absorption peak 895 nm), fabricated by organometallic synthesis [21]. PbS NC films were deposited by spin-coating followed by ligand exchange of the initial oleic acid for EDT and TBAI. To do this, PbS NCs were transferred into an octane solution, TBAI was dissolved in methanol (15 mg TBAI per 1 ml of methanol), and EDT was dissolved in acetonitrile (0.1% solution). After that, the PbS NC solution was deposited on a rotating substrate using the spin-coater method to replace by PbS NC layer for 30 c a solution of the corresponding ligands was applied, and then washed off with acetonitrile — it was also applied to 30 s, and then the substrate was spun again. The whole procedure

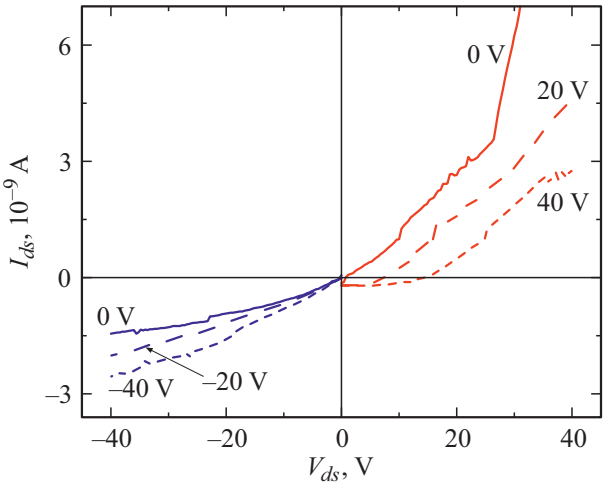

Figure 1. Output characteristics of PbS−TBAI NC film in air.

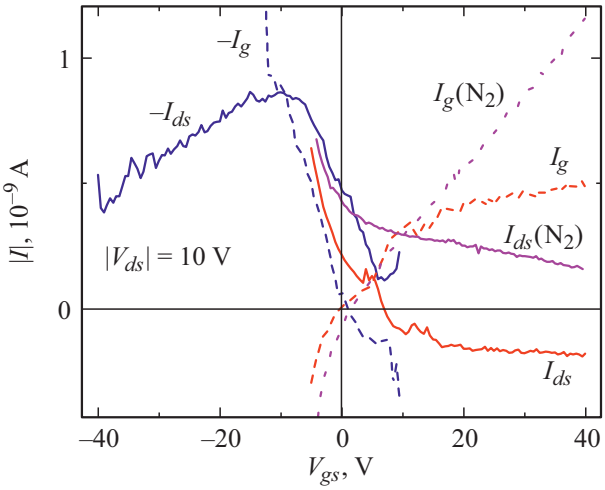

Figure 2. Transfer characteristic of PbS−TBAI NC film in air and in an inert medium (N_2)

was repeated 3 times to obtain film with a thickness of 70−80 nm.

The substrate surface was preliminarily silanized with HMDS, for which the substrate was kept for 20 min in HMDS solution (0.1 ml HDMS per 4 ml cyclohexane), after which it was washed with cyclohexane.

The study of PbS−TBAI NC films was first carried out in ambient air. Saturation is not observed in the output characteristics, and the operation proceeds in a linear mode over the entire voltage range (Fig. 1). In the region of positive bias, as the gate voltage increases, the current drops noticeably; in the region of negative bias slightly increases, i.e. in both cases, signs of hole conductivity are demonstrated. The asymmetry of the output characteristics, when the current in the positive part is higher even at zero voltage at the gate, is caused by the influence of the gate field on the channel and on the drain contact, and disappears when the gate is disconnected.

Transfer characteristics were obtained at voltage $V_{ds} = 10$ V (Fig. 2). On the *n*-channel characteristic there are no growth areas, the current drops and goes in the negative direction. The key to understanding the negative current at positive drain voltage is the current registered in the gate, which is almost a mirror of the current in the channel, and at the same time exceeds the possible leakage current by an order of magnitude. If we exclude the option of the insulator breakdown (when the current is linear, much higher and the same in both *p*- and *n*-channel characteristics), then it is obvious that the „channel−gate“ capacitance is charged. In this case, electrons fill the acceptor states (in silicon oxide or other acceptor states), causing a mirror influx of a positive charge into the gate on the other side of the insulator. In this case, there is no current in the channel, except for the capacitance charging current.

On the *p*-channel characteristic a linear growth section is observed, starting already at a positive bias $V_{\text{th-h}} = 6.5$ V, reaching saturation after $V_{gs} = -6$ V and starting to drop after −15 V. At this voltage the current registered in the gate contact exceeds the current in the channel, and, according to its sign, the gate is rapidly negatively charged. Most likely, after reaching saturation, a significant positive charge accumulates at the interface between the NC layer and the insulator, which prevents the effect of the gate and the current flow. This is shown as the negative current decreasing in the channel. At increased voltage $V_{ds} = 20$ V the linear character remains until the bias value $V_{gs} = -40$ V, which indicates that the selected section is not the inflection point. The calculated mobility was $3.0 \cdot 10^{-5}$ cm^2/(B · c), which is in the range of literature data, where the mobility can be from $2 \cdot 10^{-7}$ [22] to $2 \cdot 10^{-3}$ [23], although this is below the more common value of $\sim 10^{-4}$ cm^2/(B · c) [24,25].

The transfer of the deposition and measurement procedure to the inert environment of the glove box did not lead to a significant change in the picture, with one notable exception: on the *n*-channel characteristic the channel current I_{SD} decreases upon bias increasing, but does not go into the negative part, and the gate current now increases linearly (see Fig. 2). Thus, now „mirror“ charging of channel and gate does not occur, and the current drop may already mean simply the absence of electron conductivity, although this does not exclude the presence of a screening effect that does not allow registration of electrons mobility.

The output characteristics obtained for PbS−EDT NC films show independence from the gate voltage. Almost the same can be said about the transfer characteristics shown in Fig. 3, — the current in the channel decreases regardless of the polarity of the gate voltage, and the current through the gate I_g is comparable to the current through the channel I_{sd}. Add that at a low rise rate of gate voltage the current drops to a minimum already at low voltages, i.e. the channel is isolated from the influence of the gate potential, and this again can be explained by the formation of a charge region induced by the gate field located at the channel interface with dielectric layer. But if such behavior

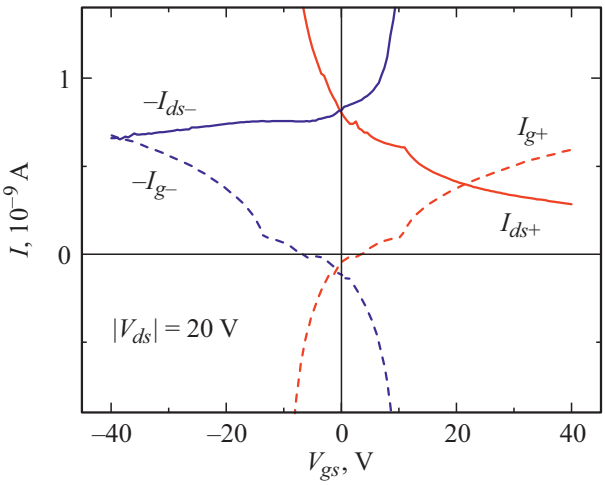

Figure 3. Transfer characteristic of PbS–EDT NC film in air.

in the n-channel conductivity region can be explained by acceptor states of silicon oxide, then the behavior in the *p*-channel conductivity region can be explained only when trap donor states are formed in the NC layer itself.

In air, the NK PbS–EDT sample did not allow obtaining any output characteristics the very next day, while the sample with TBAI showed transfer characteristics after a few more days, albeit with deteriorating parameters.

2.5. Study in the light

PbS–EDT NC layer is usually used as an electron blocking layer and is made thin (to block electrons but not to introduce excessive resistive losses). Therefore, the lack of electron conductivity is not a problem. In the PbS–TBAI NC layer, on the contrary, the formation of electron-hole pairs and their separation by the field occur; therefore, both types of conductivity should be observed. The processes in the NC layers in the light differ from the processes in the dark in that in the first case more charge carriers are formed, and the traps — if they are relatively shallow — are activated, and charges are released. In this case, the appearance of additional photoactivated carriers may show that the assumptions about the absence of electron or hole conductivity are premature. To do this, we tested the behavior of samples processed by EDT and TBAI when illuminated with a solar radiation simulator based on a xenon lamp [26].

The radiation intensity in the simulator is 100 mW/cm^2 (spectrum AM1.5G), the simulator was used together with a ZhS11 light filter to remove radiation with a wavelength shorter than 400 nm from the spectrum, since it quickly damaged the samples. To attenuate the light flux we used a glass neutral light filter HC7 and two photometric grids with a transmission of 25 and 50%. As a result, by successively adding HC7 light filter and grids, we obtained illumination of 87, 32, 8, and 4% of the initial intensity of the simulator when studying PbS–TBAI NC films and 87, 32, and 4% when studying NC PbS–EDT films.

An analysis of the change in the slope of the transfer characteristic of the PbS–TBAI NC sample in the *p*-channel conductivity region with increased illumination (see Fig. 4) shows that the mobility increased by 4 times (from $1.37 \cdot 10^{-4}$ to $5.39 \cdot 10^{-4}$ cm^2/(B · c)), and the current increased by 3.2 times. Thus, since the conductivity is defined as $\sigma = qn\mu$, where q is elementary charge, n is carriers concentration and μ is mobility, the main contribution to conductivity increasing belongs to the mobility increasing.

In the region of *n*-channel conductivity the current decreases with gate voltage increasing at all illumination levels, but the total current level increases with illumination, as the gate current does, while the gate current is lower

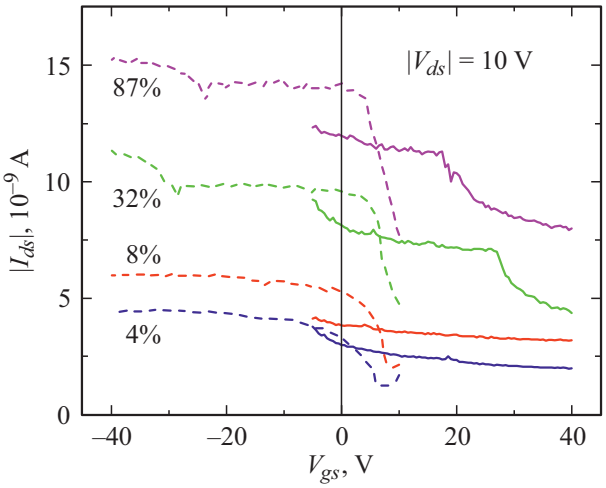

Figure 4. Transfer characteristics of PbS–TBAI NC samples. The gate current at $V_{GS} = -40$ V in the entire illumination range was 0.9 nA and therefore is not shown. At $V_{GS} = 40$ V, the gate current changes according to the change in illumination from 0.8 to 2.8 nA.

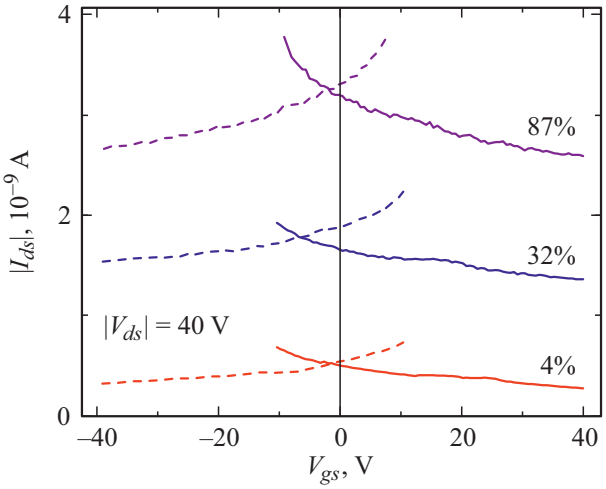

Figure 5. Transfer characteristics of PbS–EDT NC samples under illumination.

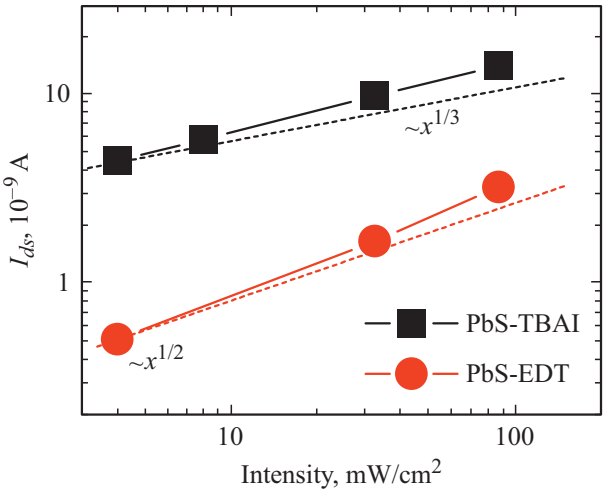

Figure 6. Current of PbS−TBAI/EDT NC samples vs. illumination. The dashed lines show the slope of the power function with exponent 1/2 and 1/3.

than the current in the channel by 2−3 times, i. e. the traps are charged, but this affects the conductivity in the channel much less than in the dark.

In the PbS−EDT NC samples, the current through the channel increases in both polarities equally with illumination increasing (Fig. 5), in the transfer characteristics a response to the gate is not observed, and the gate current practically does not increase with a change in illumination, i.e. new vacancies are not formed during illumination.

Let's pay attention to two features. Firstly, since the current in the channel is the same in both directions, and it can be assumed that the channel is shielded, and free charge carriers are not affected by the gate, we can assume that the same charge carriers participate in both polarities (but they can not be identified here). Secondly, it is interesting that the illumination of samples with EDT even with 4% intensity improves the conductivity so much that the current in the channel becomes much higher than the charging current of the gate capacitance, while the latter does not change so significantly with illumination increasing — from 0.26 to 0.5 nA (in the dark it was 0.1 nA). It is likely that when illuminated, the mobility of charge carriers increases noticeably, and they participate more in the formation of current in the channel than fall into traps, thus not causing a significant charge of the capacitance of the field-effect transistor.

Now consider the conductivity dependence on illumination. In the case of a semiconductor, this dependence is described by a power law, and ideally the exponent is 1, but due to the influence of traps, the exponent usually decreases to fractions of unity [27]. For PbS−EDT sample the current, and hence the conductivity, increases in proportion to exponent 0.60, which is close to 1/2 (see Fig. 6). For PbS−TBAI image the exponent is 0.37, which is $\sim 1/3$. This is an indirect confirmation that NC PbS−EDT have an oxidized surface, since the exponent 1/3 means surface-dominant conductivity, and 1/2 is the conductivity of the solid body [28], and the transition from the dependence 1/3 to 1/2 occurs due to the surface oxidation of the nanocrystals, in which the appearing surface traps immobilize the photocurrent charges.

In total, under illumination the conductivity of the PbS−TBAI NC layer increased by 14 times (in the dark the current was 10^{-9} A), which is close to the indicators from the article [6], where the conductivity increased by 30−60 times at illumination of 300 mW/cm^2, since if the illumination increased by 3 times, the conductivity would eventually increase by 24 times. In the case of PbS−EDT the conductivity increased more strongly, but the current was generally smaller.

3. Discussion of results

For PbS−TBAI NC samples, the holes mobility was measured, the threshold voltage V_{TH} is $\sim 5-10$ V and indicates a small polarization of the dielectric or the interface with it, a difference is also visible in samples made without and with air access. Due to the formation of trap states, the PbS−EDT NC samples, regardless of the manufacturing conditions, did not allow us to estimate the type of conductivity. At the same time, polarization ceases to be the dominant process already at a low illumination level. It was also shown in experiment with illumination that the photoconductivity of PbS−EDT NC samples is significantly affected by surface trapping states.

In general, the paper confirms the conclusions of other researchers that the PbS−EDT NC layer is a weak point of the solar cells of the structure under consideration [3]. For this reason, it is desirable to replace EDT ligands in solution rather than after deposition [29]. The recommended replacement for EDT ligands are halide ligands (chlorine and fluorine) due to less volatility, toxicity and greater stability [30].

Let us provide the reasons that made it impossible to analyze the mobility of charge carriers in the samples. For example, these could be acceptor traps in the insulator layer, which shield the gate field and prevent recording the electron mobility. But the substrate surface was treated with the same HMDS silane as in the study [20], where the turn-on voltage V_{th} was ~ 30 V. Therefore, a more probable cause is trap states on the surface of the nanocrystals themselves or at the interface with the surface of the insulator, which also cause the shielding effect. At the same time, if in the case of PBS−TBAI NCs these are acceptor states, may be occurred due to surface oxidation, then in the case of PbS−EDT NCs trap donor states are added. This is a very undesirable effect, since the PbS−EDT NC layer is used as a hole transport layer, and this can cause deterioration in the performance of devices based on them.

It is possible that, in addition to worsening of the surface passivation (which leads to NC oxidation and doping of *p*-type), additional traps are formed due to the EDT itself, especially if it is poorly washed out of the NC layer [31]. Research in the paper [6] shows that the problem may relate to EDT itself, which decomposes in air. The low-quality replacement version was considered separately, the ligand replacement procedure was analyzed, and no violations were found. Since incomplete replacement of ligands leads to increased resistance, we compared the resistivity of the samples. It was equal to $12-25\,\mathrm{kOhm}\cdot\mathrm{m}$ and is in the range of data published in the literature $5-40\,\mathrm{kOhm}\cdot\mathrm{m}$ [5,30,32].

To exclude the possibility that the substrate itself does not allow registration of electronic conductivity, the mobility in ZnO NC layer (manufactured by Sigma-Aldrich) was measured on it in air. The measurement showed electronic conductivity and a rather low value V_{th} ($< 10\,\mathrm{V}$). This confirms that the substrate with silicon oxide insulator can be used to analyze the electronic conductivity during silanization.

4. Conclusion

It is shown in the paper that for PbS NCs in air the predominant type is hole conductivity for both types of ligands, even for PbS−TBAI NCs, which should show electron conductivity in air. It is obvious that the description of SC operation in air will differ markedly from that of encapsulated elements. When analyzing the transfer characteristics, special attention is paid to the gate current, which indicates the charge accumulation in the channel. It is shown that, in the case of PbS−EDT NC films, trap donor states are formed, hindering hole conductivity. A study of the illumination effect on photoconductivity showed a different mechanism of conductivity in PbS NC layers with TBAI and EDT ligands, presumably due to surface oxidation of the latter.

Funding

This study was financially supported by the Russian Science Foundation (project No. 19-13-00332).

Conflict of interest

The authors declare that they have no conflict of interest.

References

[1] Y. Liu, M. Gibbs, J. Puthussery, S. Gaik, R. Ihly, H.W. Hillhouse, M. Law. Nano Lett., **10**, 1960 (2010).
[2] P.R. Brown, D. Kim, R.R. Lunt, N. Zhao, M.G. Bawendi, J.C. Grossman, V. Bulović. ACS Nano, **8**, 5863 (2014).
[3] W. Gao, G. Zhai, C. Zhang, Z. Shao, L. Zheng, Y. Zhang, Y. Yang, X. Li, X. Liu, B. Xu. RSC Adv., **8**, 15149 (2018).
[4] A.P. Litvin, P.S. Parfenov, E.V. Ushakova, A.V. Fedorov, M.V. Artemyev, A.V. Prudnikau, V.V. Golubkov, A.V. Baranov. J. Phys. Chem. C, **117**, 12318 (2013).
[5] I.D. Skurlov, I.G. Korzhenevskii, A.S. Mudrak, A. Dubavik, S.A. Cherevkov, P.S. Parfenov, X. Zhang, A.V. Fedorov, A.P. Litvin, A.V. Baranov. Materials (Basel), **12**, 3219 (2019).
[6] J.M. Luther, M. Law, Q. Song, C.L. Perkins, M.C. Beard, A.J. Nozik. ACS Nano, **2**, 271 (2008).
[7] A.A. Babaev, P.S. Parfenov, D.A. Onishchuk, A. Dubavik, S.A. Cherevkov, A.V. Rybin, M.A. Baranov, A.V. Baranov, A.P. Litvin, A.V. Fedorov. Materials (Basel), **12**, 4221 (2019).
[8] I.G. Korzhenevskii, D.A. Onishchuk, A.A. Babaev, A. Dubavik, P.S. Parfenov, A.P. Litvin. Semiconductors, **53**, 1946 (2019).
[9] L. Hu, A. Mandelis, X. Lan, A. Melnikov, S. Hoogland, E.H. Sargent. Sol. Energy Mater. Sol. Cells, **155**, 155 (2016).
[10] X. Yang, L. Hu, H. Deng, K. Qiao, C. Hu, Z. Liu, S. Yuan, J. Khan, D. Li, J. Tang, H. Song, C. Cheng. Nano-Micro Lett., **9**, 24 (2017).
[11] H. Wang, S. Yang, Y. Wang, J. Xu, Y. Huang, W. Li, B. He, S. Muhammad, Y. Jiang, Y. Tang, B. Zou. Org. Electron., **42**, 309 (2017).
[12] V. Podzorov. MRS Bull., **38**, 15 (2013).
[13] J. Chang, Z. Lin, C. Zhang, Y. Hao. In: *Differ. Types Field−Effect Transistors−Theory Appl.* (InTech, 2017).
[14] V. Podzorov, M.E. Gershenson, C. Kloc, R. Zeis, E. Bucher. Appl. Phys. Lett., **84**, 3301 (2004).
[15] H.H. Choi, K. Cho, C.D. Frisbie, H. Sirringhaus, V. Podzorov. Nature Materials, **17**, 2 (2018).
[16] C. Pérez-Fuster, J.V. Lidón-Roger, L. Contat-Rodrigo, E. García-Breijo. J. Sensors, **2018**, 1 (2018).
[17] Y.Y. Illarionov, G. Rzepa, M. Waltl, T. Knobloch, A. Grill, M.M. Furchi, T. Mueller, T. Grasser. 2D Mater., **3**, 035004 (2016).
[18] A. Daus, C. Vogt, N. Munzenrieder, L. Petti, S. Knobelspies, G. Cantarella, M. Luisier, G.A. Salvatore, G. Troster. IEEE Trans. Electron Dev., **64**, 2789 (2017).
[19] M.I. Nugraha, R. Häusermann, S.Z. Bisri, H. Matsui, M. Sytnyk, W. Heiss, J. Takeya, M.A. Loi. Adv. Mater., **27**, 2107 (2015).
[20] M.I. Nugraha, H. Matsui, S.Z. Bisri, M. Sytnyk, W. Heiss, M.A. Loi, J. Takeya. APL Mater., **4**, 116105 (2016).
[21] M.A. Hines, G.D. Scholes. Adv. Mater., **15**, 1844 (2003).
[22] M.J. Speirs, D.N. Dirin, M. Abdu-Aguye, D.M. Balazs, M.V. Kovalenko, M.A. Loi. Energy Environ. Sci., **9**, 2916 (2016).
[23] S.Z. Bisri, C. Piliego, M. Yarema, W. Heiss, M.A. Loi. Adv. Mater., **25**, 4309 (2013).
[24] K. Lu, Y. Wang, Z. Liu, L. Han, G. Shi, H. Fang, J. Chen, X. Ye, S. Chen, F. Yang, A.G. Shulga, T. Wu, M. Gu, S. Zhou, J. Fan, M.A. Loi, W. Ma. Adv. Mater., **30**, 1707572 (2018).
[25] Q. Lin, H. J. Yun, W. Liu, H.-J. Song, N.S. Makarov, O. Isaienko, T. Nakotte, G. Chen, H. Luo, V.I. Klimov, J.M. Pietryga. J. Am. Chem. Soc., **139**, 6644 (2017).
[26] A.P. Litvin, I.D. Skurlov, I.G. Korzhenevskii, A. Dubavik, S.A. Cherevkov, A.V. Sokolova, P.S. Parfenov, D.A. Onishchuk, V.V. Zakharov, E.V. Ushakova, X. Zhang, A.V. Fedorov, A.V. Baranov. J. Phys. Chem. C, **123**, 3115 (2019).

[27] Y. Aoyagi, K. Masuda, S. Namba. J. Appl. Phys., **43**, 249 (1972).
[28] P. Irkhin, H. Najafov, V. Podzorov. Sci. Rep., **5**, 15323 (2015).
[29] J.L. Peters, J.C. van der Bok, J.P. Hofmann, D. Vanmaekelbergh. Chem. Mater., **31**, 5808 (2019).
[30] D. Bederak, D.M. Balazs, N.V. Sukharevska, A.G. Shulga, M. Abdu-Aguye, D.N. Dirin, M.V. Kovalenko, M.A. Loi. ACS Appl. Nano Mater., **1**, 6882 (2018).
[31] R. D. Septianto, L. Liu, F. Iskandar, N. Matsushita, Y. Iwasa, S.Z. Bisri. NPG Asia Mater., **12**, 33 (2020).
[32] K.S. Jeong, J. Tang, H. Liu, J. Kim, A.W. Schaefer, K. Kemp, L. Levina, X. Wang, S. Hoogland, R. Debnath, L. Brzozowski, E.H. Sargent, J.B. Asbury. ACS Nano, **6**, 89 (2012).